Double photoionization and ionization excitation of the metastable helium *S* states

Hugo W. van der Hart, Kurt W. Meyer, and Chris H. Greene
Department of Physics and JILA, Campus Box 440, University of Colorado, Boulder, Colorado 80309-0440
(Received 5 December 1997)

Theoretical double photoionization cross sections are predicted for He initially in the $1s2s\ ^1S$ or ^3S state. The probability for double photoionization is a factor of 6 higher for the ^1S state at 20 eV above the threshold for double ionization and a factor of 3 larger at 80 eV above threshold. We compare these results with each other and with predictions for the high-energy limit to assess the influence of exchange on the double ejection process. Similar comparisons are also made for the process of photoionization-induced excitation of $He^+(n)$. [S1050-2947(98)09505-5]

PACS number(s): 32.80.Fb, 31.50.+w

I. INTRODUCTION

The nonseparable motion of the electron pair in a two-electron atom derives from their electrostatic repulsion. In a perturbative scheme that starts from an independent-electron picture, the radiative transition operator acts only on a single electron. Observation of a multielectron excitation thus probes the way in which this energy, initially donated to a single electron, becomes distributed among all excited electrons. A particularly sharp probe of correlations that has received increasing attention in recent years is the probability for ejection of two electrons following the absorption of a single photon.

Helium has served as *the* benchmark atom for accurate tests of double photoionization cross sections by theoretical and experimental groups. Several recent experimental results exist for the ratio between double and single ionization [1–3] and the probability for single photoionization with excitation of the residual He^+ ion has also been examined [4]. Although theoretical studies of double photoionization were initiated at least three decades ago [5], subsequent studies were rare (see, e.g., [6]), until the recent improvements in experimental capabilities. In the past five years, numerous theoretical techniques have been used to calculate the ratio of double photoionization and single photoionization probabilities for photons incident on the ground state of helium [7–14]. Earlier approaches struggled to obtain agreement between different gauge choices for the radiation field, but the most recent calculations have solved those difficulties. The agreement between theory and experiment is now very good, in part because the experimental measurements have improved substantially during the same time period. In one of the more recent developments, good agreement between theory and experiment has also been obtained for the probability for photoionization-induced excitation (PIE) of the residual $He^+(n)$ ion, with $n=2-6$ [12,14].

While the ejection of two electrons from the ground state probes the influence of correlation in the photoionization process, even more dramatic influences of the electron interactions are revealed in excited-state photoionization. The electrostatic repulsion can only shift the energy of the $1s^2$ configuration. On the other hand, the $1s2s$ configuration is not only shifted in energy by this interaction, it is also split into a nondegenerate singlet and triplet state, for which the spin-angular exchange matrix elements of the $1/r_{12}$ potential differ in sign. Differences between the double photoionization and PIE spectra for these two states thus measure the role of exchange in the two-electron dynamics. Some theoretical effort has already been invested in calculations for the $1s2s\ ^3S$ state in the limit of ''infinite'' nonrelativistic energies [15]; angular distributions have also been calculated from near threshold up to several keV beyond [16].

Exciting experimental possibilities have recently been opened up by the availability of high-intensity and high-resolution synchrotron light sources. This should make it possible to test the predictions presented here, despite the fact that both of the $1s2s$ states are only metastable. The singlet state decays mainly by spontaneous two-photon emission to the $1s^2$ ground state and has a lifetime of 19.7 ± 1.0 ms [17]. The ^3S state decays by an $M1$ transition to the ground state and has a lifetime greater than 10^4 s. Both lifetimes are (in principle) sufficiently long to allow experimental measurements, though such an experiment is clearly far more difficult than ground-state photoionization.

In the sections below, we report our calculated ratios between the double and single photoionization cross sections for the $1s2s\ ^1S^e$ and $^3S^e$ states, at final state energies up to 80 eV beyond threshold. Some of the effects arising from the difference in initial states can be estimated using explicit analytical formulas that were derived for the (nonrelativistic) high-frequency limit [18,19]. This limit not only provides a check for our calculations, but it also conveys information about the role of exchange effects. The PIE cross sections for photoexcitation of the residual ion are also reported for both initial states and compared with their high-frequency limits.

II. THEORETICAL APPROACH

We adopt the same R-matrix approach employed recently to determine the ratio of double and single photoionization cross sections [11] and the single excitation PIE cross sections [14] for ground-state helium. The calculation utilizes a finite-element description of the helium electrons within a finite reaction volume whose radius r_0 has been varied from 14 to 20 a.u. in the present study. The finite elements used here consist of a set of six fifth-order Hermite polynomials. For a more extensive discussion of the basis set, including its adaptation to double-escape problems, the reader is referred

to [11,20,21]. The radial configuration space for each electron is divided into 16 elements, which yields a total of 64 independent single-electron wave functions for each angular momentum, after taking continuity conditions between adjacent elements into account. In addition, for each ℓ value, the 16 lowest eigenfunctions of these 64 have been included in the calculations as target states for single and double ionization channels through inclusion of nonvanishing finite elements at the boundary of the box. Four elements are chosen to have a length of 0.5 a.u. between $r=0$ and 2 a.u., while each additional element at larger radii has a length of either 1 or 1.5 a.u. This mesh density is adequate to determine approximate cross sections for all energetically allowed processes up to a final-state energy 80 eV above the double ionization threshold. For the initial state, all partial waves up to d electrons are included, while for the final state f electrons are included as well. The ratios for double and single photoionization have been determined in the length, velocity, and acceleration representations for the light-matter interaction. The velocity and acceleration gauge results agree generally within 1%. However, the length and acceleration results agree within 2% for a box size of 20 a.u., but the difference increases to 20% for a box size of 14 a.u. The PIE cross sections for $He^+(n)$ are in good agreement for the velocity and acceleration gauge, although the latter appears to be somewhat better converged.

Since a finite-element basis set is employed, discrete states are obtained within the box. Apart from the lowest states, which are contained within the box, the other states do not represent physical eigenstates of the Hamiltonian in infinite volume. The ability of this scheme to obtain reasonable results hinges on the short-range nature (except at the double escape threshold) of the photoionization process (see, e.g., [14]), which allows us to describe the dominant physics within a finite reaction volume. A frame transformation [22] is then used to superpose excitation amplitudes for different discrete box states *coherently*, which yields the amplitudes for production of physical He^+ eigenstates. Previous comparisons with ground-state experiments (and other theoretical results) have shown that this method determines reliable double photoionization and PIE cross sections in the intermediate-energy range where the cross sections are largest. Somewhat surprisingly, as has been detailed elsewhere [14], the cross sections are accurate even for the production of high-lying $He^+(n)$ Rydberg states, whose radial extents exceed the size of the R-matrix box considerably.

Some residual oscillations remain in any observables calculated for a single fixed box radius, but these artifacts rapidly diminish when the cross sections are calculated at a handful of different box radii and then averaged. In this paper, our calculations have been carried out for seven box sizes, $r_0=14$–20 a.u., with a step size of 1 a.u.

III. RESULTS AND DISCUSSION

We concentrate on the ratio R of double and single photoionization cross sections as our probe of differences between the $1s2s\ ^1S$ and ^3S states of He. The notion that this ratio is a good measure for the strength of correlations in the $1s2s$ initial and final states is supported by the near spin independence of our calculated single photoionization cross sections.

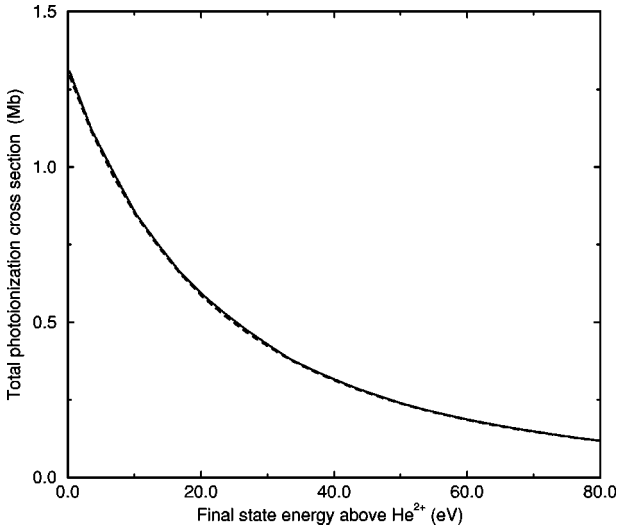

FIG. 1. Total photoionization cross sections, i.e., the sum of single and double ionization, for $1s2s\ ^1S$ (solid line) and $1s2s\ ^3S$ (dashed line) of He as a function of the final-state energy above the He^{2+} threshold.

The single photoionization cross sections for the $1s2s\ ^1S$ and ^3S states are shown in Fig. 1. The maximum difference between the single ionization cross sections is 1.5%. This confirms that the qualitative differences in the ratio R reflect differences in the electron correlation dynamics of the double escape process and/or differences in the initial-state correlations.

Exchange manifests itself both in the initial and in the final-state wave function. However, as discussed by Dalgarno and Sadeghpour [23], the determination of the single ionization cross section with excitation to the ns state in the infinite frequency limit only depends on electron correlations through the initial-state wave function (at least in the acceleration ''gauge''). The single ionization oscillator strength behaves in the infinite-frequency limit as [18]

$$\frac{df^+}{d(2\epsilon)}=C(ns)(2\epsilon)^{-7/2}\left(1-\frac{2\pi}{(2\epsilon)^{1/2}}\right), \tag{1}$$

with ϵ the photoelectron energy. The proportionality constant $C(ns)$ is then given by [19]

$$C(ns)=\frac{512\pi Z^2}{3}\left|\langle\Psi(r_1,r_2)|\,\delta(r_2)|\,\phi_{ns}(r_1)\rangle\right|^2, \tag{2}$$

with ϕ_{ns} the hydrogenic radial wave function and Ψ the initial-state wave function. The proportionality constant summed over all possible final states is given by

$$C=\frac{512\pi Z^2}{3}|\Psi(r_1,0)|^2, \tag{3}$$

so that the ratio of double to single ionization is given as

$$R=\frac{C-\Sigma_n C(ns)}{\Sigma_n C(ns)}. \tag{4}$$

Using a B-spline basis set approach, wave functions have been obtained for both $1s2s$ states using an expansion with

TABLE I. Wave-function composition of the $1s2s$ states of He.

State	$1s2s\ ^1S^e$	$1s2s\ ^3S^e$
$1s^2$	−0.1112	
$1s2s$	−0.7550	−0.8990
$1s3s$	0.6351	0.4245
$1s4s$	0.0564	0.0680
$1s5s$	0.0392	0.0377
$2s^2$	0.0077	
$2s3s$	0.0041	−0.0020
$2p^2$	0.0156	
$2p3p$	−0.0018	0.0093

all angular momenta up to $\ell=2$ included. Some coefficients of the final wave functions are reported in Table I. The difference between the singlet and the triplet state can be observed readily from the coefficients for the $1s2s$ and the $1s3s$ basis functions. The resulting values for $C(ns)$ and R have been determined and are given in Table II for the $1s2s\ ^1S^e$ and the $1s2s\ ^3S^e$ states and compared with the results obtained by Forrey *et al.* [15]. The agreement between the two sets of results is very good, with the relative differences well below 1% for both the $1s2s$ singlet and triplet states.

Noticeable differences can be observed between the infinite-energy limits for the singlet and the triplet $1s2s$ states. The stronger configuration interaction for the singlet states results in a much higher probability for leaving the He^+ ion in the $3s$ state when excited from a singlet initial state. Apart from the $2s$ state and the $4s$ state, all other states have higher probability for the singlet than for the triplet spin state. In fact, the ratio of double to single photoionization is a factor of 3 larger for the $1s2s\ ^1S^e$ state. These differences are only due to the initial state and thus reflect solely the effect of exchange on the correlation interaction.

It should be remembered that in order to obtain the infinite-frequency limit, the integrations over the initial $^1S^e$ or $^3S^e$ state in Eqs. (2) and (3) need to be carried out only over configurations containing two s electrons. The $\delta(r_2)$ function only has a contribution when the wave function has an amplitude at $r=0$. Other configurations, such as p^2, are nevertheless mixed in and affect the contributions from s^2 configurations indirectly through the normalization. These angular momenta, $\ell>0$, contribute to the ionization as well, but only at lower, finite, energies.

TABLE II. Ratios of $C(ns)/C$ and R for various states of He.

	$1s2s\ ^1S^e$		$1s2s\ ^3S^e$	
n		[15]		[15]
1	0.0493	0.0493	0.0338	0.0338
2	0.5345	0.5346	0.7824	0.7824
3	0.3993	0.3993	0.1732	0.1733
4	0.0035	0.0035	0.0044	0.0044
5	0.0017	0.0017	0.0013	0.0014
6	0.0009	0.0009	0.0006	0.0006
$C(\varepsilon s)/c$	0.00894	0.0089	0.00311	
R	0.00902	0.009033	0.00312	0.003118

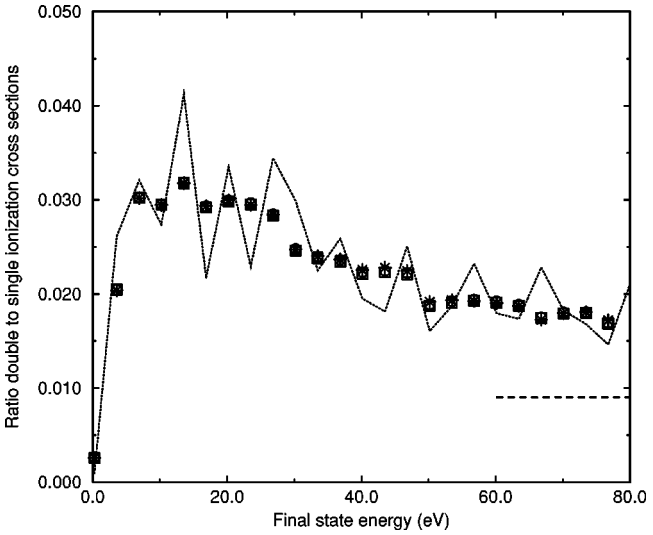

FIG. 2. Ratio of the double ionization vs the single ionization cross sections for the $1s2s\ ^1S$ state of He in the length (asterisks), velocity (open squares), and acceleration frame (open circles) using box averaging. The infinite-energy result is indicated as a horizontal dashed line from 60 to 80 eV. The acceleration frame results at a radius of 17 a.u. are given by the dotted line to illustrate the influence of the box averaging.

The double to single photoionization cross section ratios for the $1s2s\ ^1S$ and ^3S states are presented in Figs. 2 and 3, respectively. The agreement between the three different gauges is generally very good, although the length gauge is less accurately converged than the other two. For both symmetries, the infinite energy limit has not been reached at an energy of 80 eV above threshold, where a factor of 2 discrepancy remains for both symmetries. For the $1s2s\ ^1S$ state, however, it can be seen that the ratio is still decreasing;

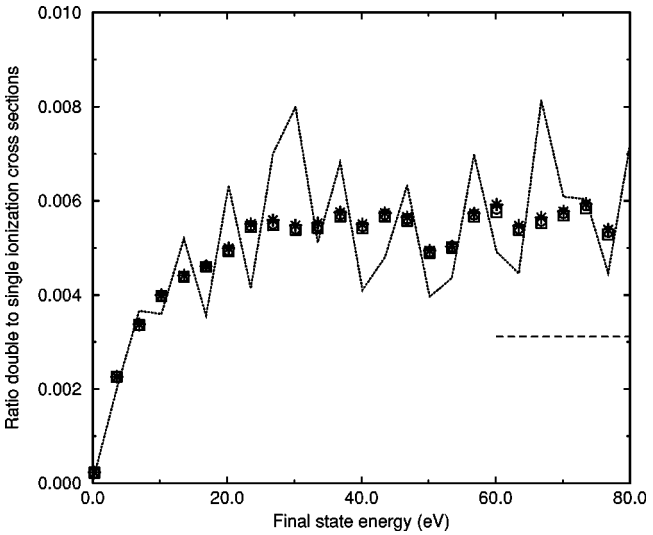

FIG. 3. Ratio of the double ionization vs the single ionization cross sections for the $1s2s\ ^3S$ state of He in the length (asterisks), velocity (open squares), and acceleration frame (open circles) using box averaging. The infinite-energy result is indicated as a horizontal dashed line from 60 to 80 eV. The acceleration frame results at a radius of 17 a.u. are given by the dotted line to illustrate the influence of the box averaging.

results at higher frequencies will be required to establish the asymptotic behavior. In the present approach, this requires significantly smaller finite elements and consequently a much larger calculation. For the $1s2s\ ^3S$ state, a plateau is reached between 40 and 80 eV (the dip at 50 eV is unphysical). For higher energies above threshold, there are preliminary indications that the cross sections indeed decrease.

The shape of the cross sections is very different. A maximum of 0.03 for the ratio of double ionization to single ionization is reached for the ^1S state at an energy of 15 eV above the double-ionization threshold, whereas for the ^3S state, a maximum of 0.0055 appears to be reached around roughly 60 eV above threshold. This different behavior is due to the difference in the exchange because the Pauli exclusion principle for a triplet state does not allow the two electrons close together in either position space or in momentum space. For lower energies near threshold, this leads to a cross section smaller for the triplet than for the singlet state.

The good agreement among our calculations with three different gauges may seem surprising, in view of the unphysical modulations in the energy-dependent spectra above the ionization threshold. In fact, it is natural because our implementation of a finite-element basis set has made our solution of the Schrödinger equation almost ''exact'' at small distances, aside from our truncation of the partial wave expansion. On the other hand, we have imposed unphysical boundary conditions at the edge of the R-matrix box, owing to our discretization of the He^+ eigenstates at an intermediate step in the calculation; that discretization is box size dependent and it causes the incorrect modulations. When the full R-matrix calculation is repeated for several different box radii and the resulting cross sections are averaged, however, the average spectrum settles down and the unphysical modulations diminish. This has been documented in our earlier papers dealing with this approach to the two-electron continuum problem [8,22].

Figures 2 and 3 provide a glimpse of the evidence that supports our assertions in the preceding paragraph because we include one spectrum calculated at a single box radius ($r_0=17$ a.u.) in addition to the box-size-averaged spectrum. Clearly, the cross sections plotted for $r_0=17$ a.u. display far larger modulations of an unphysical nature, as compared to the box-averaged results. The range of r_0 values used in the box-averaging needs to be sufficiently large so that it will sweep one of the discretized continuum states of He^+ into at least the next state with the same ℓ but one more node, for any level in the energy range of primary interest (see, e.g., Fig. 1 in [22]).

The probabilities for leaving an excited He^+ atom for the $1s2s\ ^1S$ and ^3S states are given in Figs. 4 and 5, respectively. The infinite-frequency limit is indicated by the horizontal dashed lines. For the excitation of the $n=2$ and the $n=3$ states, the present results are in very good agreement with the infinite-frequency limit, but for the higher n (4, 5, and 6) states higher frequencies have to be investigated to establish the asymptotic limits from the photoionization calculations.

The main difference between the two symmetries is observed to occur for these high-n states. Although the infinite-energy limits are quite similar for the two symmetries, the behavior as a function of energy differs significantly. At the infinite-energy limit, the excitation probabilities are larger for the triplet state by a factor 1.05–2, whereas just above the double ionization threshold, the excitation probabilities are larger for the singlet state by a factor 3–5. One reason for this difference is that contributions to the initial state with angular momentum $\geqslant 1$ are more important for the singlet states. These contributions are zero in the infinite-energy limit, but not so for finite energies.

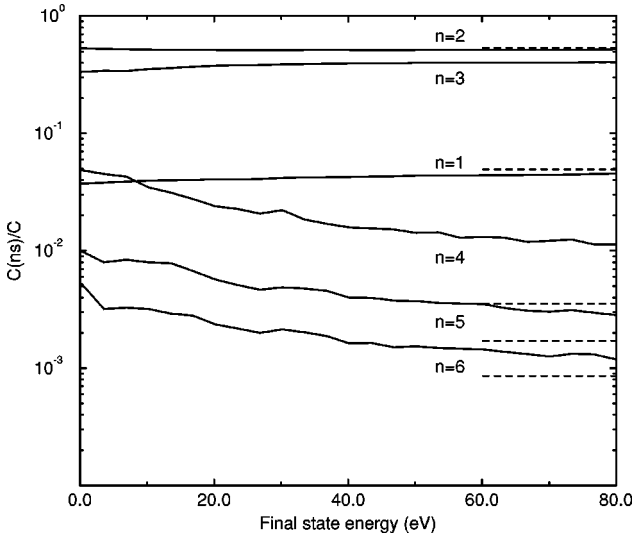

FIG. 4. Ratio of single ionization with excitation to the $n\ell$ states vs total ionization for the $1s2s\ ^1S$ state of He. The curves represent, from top to bottom at 80 eV, $n=2$, $n=3$, $n=1$, $n=4$, $n=5$, and $n=6$. The infinite-energy results for these n values are indicated as a horizontal dashed line from 60 to 80 eV.

The better agreement of the infinite-energy approach for excitation of the $n=2$ and $n=3$ states is due to the dominance of the $1s2s$ and $1s3s$ configurations in the configuration-interaction expansion. Configurations contain-

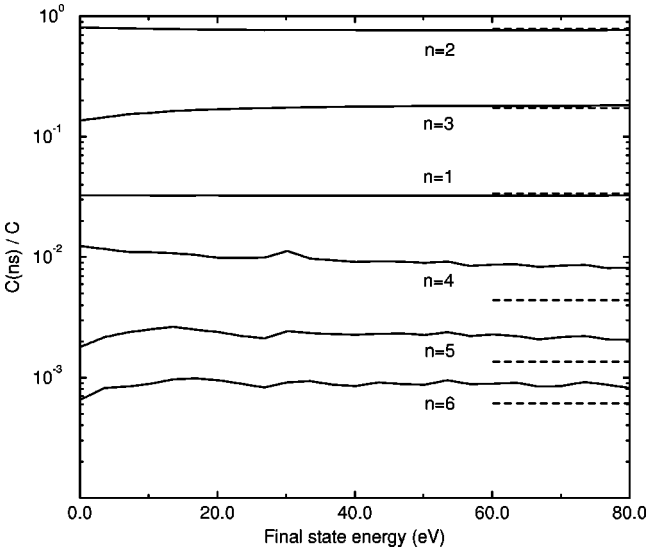

FIG. 5. Ratio of single ionization with excitation to the $n\ell$ states vs total ionization for the $1s2s\ ^3S$ state of He. The curves represent, from top to bottom at 80 eV, $n=2$, $n=3$, $n=1$, $n=4$, $n=5$, and $n=6$. The infinite-energy results for the states are indicated as a horizontal dashed line from 60 to 80 eV.

ing $2p$, $3p$, or $3d$ electrons are two orders of magnitude less important. For the higher Rydberg states, this is not the case. The contribution from configurations containing $4p$ are relatively more important.

The rate for ionization with excitation to the $n\ell$ states scales with n^{-3} for high Rydberg states. This scaling law has been verified for the infinite-frequency results for n up to 10, while the present results indicate that this n^{-3} behavior applies at finite frequencies for $n \geq 5$.

IV. CONCLUSIONS

The ratio between double and single ionization has been obtained for the $1s2s\ ^1S$ and ^3S states of He for frequencies reaching final states from 0 to 80 eV above the threshold for double ionization. Stronger correlation effects for the singlet symmetry lead to a much higher probability for double ionization for the $1s2s\ ^1S$ state, about a factor of 3 in the infinite-energy limit and a factor of 6 at a final state energy of 18 eV. The behavior of the double to single ionization ratio also differs for the two symmetries. For the singlet symmetry, a peak ratio of 0.03 is reached in a relatively narrow maximum at about 18 eV above threshold, while for the triplet symmetry a peak ratio of 0.006 is found in a broad maximum near 60 eV above threshold.

Ionization with excitation of the residual has also been investigated for both of the $1s2s$ states. The excitation of the $n=2$ and $n=3$ states shows little variation with frequency for both states and is in good agreement with the results obtained for infinite frequency. A large variation with frequency is found, however, for the excitation of the $n=4$, 5, and 6 states for an initial state $1s2s\ ^1S$. This variation is much smaller for the triplet state and is ascribed to the importance of higher angular momenta in the initial wave function, which are more prominent for the singlet symmetry.

Despite the recent interest in double photoionization processes, no experiments have been performed on these long-lived metastable excited states of helium. Experimental results for these states would help to obtain information about the influence of exchange on the double photoionization process and to assess the accuracy of the present calculations.

ACKNOWLEDGMENTS

The authors wish to thank J.L. Bohn for stimulating discussions. This work was supported by the Division of Chemical Sciences, Office of Basic Energy Sciences, Office of Energy Research, U.S. Department of Energy.

[1] J.A.R. Samson, Z.X. He, L. Yin, and G.N. Haddad, J. Phys. B **27**, 887 (1994).
[2] R. Dörner *et al.*, Phys. Rev. Lett. **76**, 2654 (1996).
[3] J.C. Levin, G.B. Armen, and I.A. Sellin, Phys. Rev. Lett. **76**, 1220 (1996).
[4] R. Wehlitz *et al.*, J. Phys. B **30**, L51 (1997).
[5] F. Byron and C.J. Joachain, Phys. Rev. **164**, 1 (1967).
[6] S.L. Carter and H.P. Kelly, Phys. Rev. A **24**, 170 (1981).
[7] L.R. Andersson and J. Burgdörfer, Phys. Rev. Lett. **71**, 50 (1993).
[8] K.W. Meyer and C.H. Greene, Phys. Rev. A **50**, R3573 (1994).
[9] J.-Z. Tang and I. Shimamura, Phys. Rev. A **52**, R3413 (1995).
[10] A.S. Kheifets and I. Bray, Phys. Rev. A **54**, R995 (1996).
[11] K.W. Meyer, C.H. Greene, and B.D. Esry, Phys. Rev. Lett. **78**, 4902 (1997).
[12] J.-Z. Tang and J. Burgdörfer, J. Phys. B **30**, L523 (1997).
[13] P.J. Marchalant and K. Bartschat, Phys. Rev. A **56**, R1697 (1997).
[14] K.W. Meyer, J.L. Bohn, C.H. Greene, and B.D. Esry, J. Phys. B **30**, L641 (1997).
[15] R.C. Forrey, H.R. Sadeghpour, J.D. Baker, J.D. Morgan III, and A. Dalgarno, Phys. Rev. A **51**, 2112 (1995).
[16] Z. Teng and R. Shakeshaft, Phys. Rev. A **49**, 3597 (1993).
[17] R.S. van Dyck Jr., C.E. Johnson, and H.A. Shugart, Phys. Rev. A **4**, 1327 (1971).
[18] P.K. Kabir and E.E. Salpeter, Phys. Rev. **108**, 1256 (1957).
[19] A. Dalgarno and A.L. Stewart, Proc. Phys. Soc. London **76**, 47 (1960).
[20] J. Shertzer and J. Botero, Phys. Rev. A **49**, 3673 (1994).
[21] J.P. Burke, C.H. Greene, and B.D. Esry, Phys. Rev. A **54**, 3225 (1996).
[22] K.W. Meyer, C.H. Greene, and I. Bray, Phys. Rev. A **52**, 1334 (1995).
[23] A. Dalgarno and H. Sadeghpour, Phys. Rev. A **46**, R3591 (1992).